Applied Materials Today 4 (2016) 45–53

Contents lists available at ScienceDirect

Applied Materials Today

journal homepage: www.elsevier.com/locate/apmt

Synthesis procedure and type of graphite oxide strongly influence resulting graphene properties

Ondřej Jankovský, Petr Marvan, Michal Nováček, Jan Luxa, Vlastimil Mazánek, Kateřina Klímová, David Sedmidubský, Zdeněk Sofer*

Department of Inorganic Chemistry, University of Chemistry and Technology Prague, Technická 5, 166 28 Prague 6, Czech Republic

ARTICLE INFO

Article history:
Received 3 June 2016
Received in revised form 24 June 2016
Accepted 25 June 2016

Keywords:
Graphene
Thermal reduction
Chemical reduction
Structure
Chemical composition

ABSTRACT

Graphene is the one of the most intensively studied materials for its unique mechanical, electrical and thermal properties. The aim of this study is to compare the significant differences between individual graphenes prepared using different graphite oxides as starting materials. Graphene was prepared by chemical and thermal reduction of five different graphite oxides, which were prepared according to Brodie, Hofmann, Hummers, Staudenmaier and Tour method. Due to the significant differences in the composition of graphite oxide used for synthesis significant differences can be also observed in graphene prepared by chemical and thermal reduction of starting material. The synthesized graphene materials were characterized in detail using different chemical and structural analytical methods. Significant level of unintentional nitrogen doping was observed on chemically reduced graphite oxide synthesized by permanganate methods. Also the degree of exfoliation and the corresponding structural properties were strongly dependant on the degree of oxidation of the starting graphite oxide. Finding the best synthesis procedure of graphene with desirable properties is essential to optimize technologies in large scale production of graphene for its utilization in industrial applications.

1. Introduction

Due to its unique electrical, optical and mechanical properties graphene has been intensively studied since its isolation in 2004 [1–3]. These unique properties make graphene a highly promising material for a wide range of applications in modern electronics and electrochemical power sources such as supercapacitors, fuel cells or batteries which are of extreme importance for the green energy production and storage [4–9]. Thanks to extremely high surface area, graphene also seems to be useful for removal of toxic contaminants from environment [10–12]. A number of various methods for the synthesis of graphene have been reported. One possibility how to obtain graphene directly is the mechanical exfoliation of graphite [13], other common methods are CVD techniques [14]. CVD-based graphene layers are of large size, high-quality and they are important for optoelectronic or microelectronic devices. However, for applications in the field of electrochemical power sources and composites, graphene should be produced in larger amounts [15–17]. For this purpose, the reduction of graphite oxide seems to be the most suitable method. In this method graphite precursor is oxidized in acidic environment using chlorate or permanganate methods to graphite oxide. Subsequently, the formed graphite oxide is reduced by different routes yielding graphene. Graphite oxide can be reduced using microwaves [18], by ion bombardment [19], or by chemical or thermal reduction [20,21]. Various reducing agents for the chemical reduction have been reported from which the most common are hydrazine and its derivatives [20], hydroquinone [22], complex hydrides [23] or nascent hydrogen [24–26]. Graphite oxide can be also reduced thermally in inert (nitrogen) or reducing atmosphere (hydrogen). The thermal reduction of graphite oxide produces graphene with the highest degree of exfoliation and also largest surface area [27,28]. The thermal reduction is usually performed by rapid heating in suitable non-oxidizing atmosphere. The mechanism of the thermal reduction has been described as a process of decomposition of oxygen containing functional groups forming carbon dioxide, carbon monoxide and water during the heating. The evolved gaseous products increase interlayer pressure, which eventually leads to the exfoliation. However, a few papers described that the process is much more complex accompanied by a release of more complex species during exfoliation [29,30].

In this study, we investigated in detail the influence of starting graphite oxide preparation method on the composition, structure and properties of thermally and chemically reduced graphene. For these syntheses we selected the methods which can be easily scaled

* Corresponding author.
E-mail address: zdenek.sofer@vscht.cz (Z. Sofer).

http://dx.doi.org/10.1016/j.apmt.2016.06.001
2352-9407/

up for industrial production using rapid thermal exfoliation in nitrogen atmosphere and chemical reduction using hydrazine in alkaline environment. For the synthesis of graphite oxides the chlorate based methods (Brodie, Staudenmaier and Hofmann method) and permanganate methods (Hummers and Tour method) were applied. Chemical composition of the obtained products was investigated in detail using X-ray photoelectron spectroscopy (XPS) and elemental combustion analysis. The structural properties were investigated by scanning electron microscopy (SEM), Raman spectroscopy, X-ray diffraction (XRD), surface area measurement (BET method) and the thermal stability towards oxidation was probed by simultaneous thermal analysis (STA). In addition basic electrochemical properties were investigated using cyclic voltammetry and various redox probes.

2. Experimental

We prepared five different graphite oxides from pure graphite microparticles (2–15 μm, 99.9995%) from Alfa Aesar, Germany. Sulphuric acid (98%), nitric acid (68%), fuming nitric acid (>98%), potassium chlorate (99%), potassium permanganate (99.5%), sodium nitrate (99.5%), hydrogen peroxide (30%), hydrochloric acid (37%), silver nitrate (99.5%), phosphoric acid (85%), barium nitrate (99.5%), potassium hydroxide (>99.9%), hydrazine hydrate (99%), methanol (>99.9%) and N,N-dimethylformamide (DMF) were obtained from Penta, Czech Republic. Nitrogen (99.9999%) was obtained from SIAD, Czech Republic.

Graphite oxide prepared by the Brodie method was termed BR-GO [31]. Fuming nitric acid (>98%, 62.5 mL) was added to a reaction flask containing a magnetic stir bar. The mixture was then subsequently cooled to 0 °C and graphite (5 g) was added. The mixture was stirred to obtain a homogeneous dispersion. While keeping the reaction flask at 0 °C, potassium chlorate (25 g) was slowly added to the mixture. Upon the complete dissolution of potassium chlorate, the reaction flask was loosely capped to allow the escape of the gas evolved and the mixture was stirred for 20 h at 40 °C. Upon completion of the reaction, the mixture was poured into 3 L of deionized water and decanted. Graphite oxide was then redispersed in HCl solution (5%, 3 L) to remove sulphate ions and repeatedly centrifuged and redispersed in deionized water until a negative reaction on chloride ions was achieved. Graphite oxide slurry was then dried in a vacuum oven. The composition obtained by elemental combustion analysis was 59.99 at.% C, 23.06 at.% O, 16.82 at.% H and 0.13 at.% N. More details are given in Supporting Information.

Graphite oxide prepared according to the Hofmann method was termed HO-GO [32]. Sulphuric acid (98%, 87.5 mL) and nitric acid (68%, 27 mL) were added to a reaction flask (Pyrex beaker with thermometer) containing a magnetic stir bar. The mixture was then cooled by immersion in an ice bath for 30 min. Graphite (5 g) was then added to the mixture with vigorous stirring motion. While keeping the reaction flask in the ice bath, potassium chlorate (55 g) was slowly added to the mixture. Upon the complete dissolution of potassium chlorate, the reaction flask was then loosely capped to allow the escape of the gas evolved and the mixture was continuously stirred for 96 h at room temperature. The mixture was poured into 3 L of deionized water and decanted. Graphite oxide was then redispersed in HCl solution (5%, 3 L) to remove sulphate ions and repeatedly centrifuged and redispersed in deionized water until a negative reaction on chloride and sulphate ions was achieved. Graphite oxide slurry was then dried in a vacuum oven. The composition obtained by elemental combustion analysis was 47.45 at.% C, 28.81 at.% O, 23.71 at.% H and 0.02 at.% N. More details are given in Supporting Information.

The third graphite oxide was synthesized similarly to the Hummers method and was termed as HU-GO [33]. Graphite (5 g) and sodium nitrate (2.5 g) were stirred with sulphuric acid (98%, 115 mL). The mixture was then cooled to 0 °C. Potassium permanganate (15 g) was then added over a period of 2 h. During the next 4 h, the reaction mixture was allowed to reach room temperature before being heated to 35 °C for 30 min. The reaction mixture was then poured into a flask containing deionized water (250 mL) and heated to 70 °C for 15 min. The mixture was then poured into deionized water (1 L). The unreacted potassium permanganate and manganese dioxide were removed by the addition of 3% hydrogen peroxide. The reaction mixture was then allowed to settle and decant. The obtained graphite oxide was then purified by repeated centrifugation and redispersing in deionized water until a negative reaction on sulphate ions was achieved. Graphite oxide slurry was then dried in a vacuum oven. The composition obtained by elemental combustion analysis was 41.38 at.% C, 31.80 at.% O, 26.80 at.% H and 0.02 at.% N. More details are given in Supporting Information.

Graphite oxide prepared by the Staudenmaier method was termed ST-GO [34]. Sulphuric acid (98%, 87.5 mL) and fuming nitric acid (>98%, 27 mL) were added to a reaction flask containing a magnetic stir bar. Subsequently, the mixture was cooled to 0 °C and graphite (5 g) was added. The mixture was vigorously stirred to avoid agglomeration and to obtain a homogeneous dispersion. While keeping the reaction flask at 0 °C, potassium chlorate (55 g) was slowly added. Upon the complete dissolution of potassium chlorate, the reaction flask was loosely capped to allow the escape of the gas evolved. Then the mixture was continuously stirred for 96 h at room temperature. The mixture was then poured into deionized water (3 L) and decanted. Graphite oxide was redispersed in HCl solution (5%, 3 L) to remove sulphate ions and repeatedly centrifuged and redispersed in deionized water until a negative reaction on chloride and sulphate ions was achieved. Graphite oxide slurry was then dried in a vacuum oven. The composition obtained by elemental combustion analysis was 70.47 at.% C, 17.94 at.% O, 11.34 at.% H and 0.25 at.% N. More details are given in Supporting Information.

The last graphite oxide prepared according to the Tour method (TO-GO) [35]. Firstly the mixture of concentrated sulphuric acid and phosphoric acid in a volume ratio 9:1 (360 mL:40 mL) was cooled under 0 °C. Next we added graphite (3.0 g) and subsequently potassium permanganate (18.0 g). The ongoing reaction heated the mixture itself to 20–25 °C due to the exothermic process. The reaction mixture was stirred and then heated to 50 °C during 12 h. Then was the mixture cooled to 20 °C and poured onto to ice with hydrogen peroxide (3.0 mL) to remove an excess of permanganate ions and manganese dioxide. After the ice dissolve 30% hydrogen peroxide was added to remove remaining unreacted potassium permanganate and manganese dioxide. The obtained graphite oxide was then purified by repeated centrifugation and redispersing in deionized water until a negative reaction on sulphate ions was achieved. Graphite oxide slurry was then dried in a vacuum oven. The composition obtained by elemental combustion analysis was 34.83 at.% C, 36.23 at.% O, 28.94 at.% H and 0.00 at.% N. More details are given in Supporting Information.

Chemically reduced graphene denoted “CRG” was prepared by reduction with hydrazine hydrate. 1 g of graphite oxide was dispersed in 1 L of deionized water by ultrasonication (150 W, 60 min). The suspension was alkalized to pH 10 by 1 M KOH. 10 mL of hydrazine hydrate was added to the reaction mixture and the solution was kept under reflux for 24 h. The obtained CRG was separated from the reaction mixture by suction filtration using a nylon membrane with 0.45 μm porosity and repeatedly washed with deionized water and methanol. Prior to further use, CRG was dried in a vacuum oven at 60 °C for 48 h.

The thermal reduction–exfoliation of graphite oxide was performed at 1000 °C in quartz glass reactor in nitrogen atmosphere. Accordingly, samples were termed “TRG”. Graphite oxide (0.1 g)

was placed in a porous quartz glass capsule connected to magnetic manipulator inside vacuum tight tube furnace with controlled atmosphere. The sample was flushed with nitrogen by repeated evacuation of tube furnace to remove any traces of oxygen. Subsequently the reactor was filled with nitrogen or hydrogen, respectively and the sample was quickly inserted by magnetic manipulator in to the preheated furnace and held in the furnace for 12 min. The flow of nitrogen during the exfoliation procedure was 1000 sccm to remove the byproducts of exfoliation procedure.

The morphology was investigated using scanning electron microscopy (SEM) with a FEG electron source (Tescan Lyra dual beam microscope). Elemental composition and mapping were performed using an energy dispersive spectroscopy (EDS) analyzer (X-Max^N) with a 20 mm^2 SDD detector (Oxford instruments) and AZtecEnergy software. To conduct the measurements, the samples were placed on a carbon conductive tape. SEM and SEM-EDS measurements were carried out using a 10 kV electron beam.

Combustible elemental analysis (CHNS-O) was performed using a PE 2400 Series II CHNS/O Analyzer (Perkin Elmer, USA). The instrument was used in CHN operating mode (the most robust and interference-free mode) to convert the sample elements to simple gases (CO_2, H_2O and N_2). The PE 2400 analyzer automatically performed combustion, reduction, homogenization of product gases, separation and detection. An MX5 microbalance (Mettler Toledo) was used for precise weighing of the samples (1.5–2.5 mg per single sample analysis). Using this procedure, the accuracy of CHN determination is better than 0.30% abs. Internal calibration was performed using an N-fenyl urea.

High resolution X-ray photoelectron spectroscopy (XPS) was performed using an ESCAProbeP spectrometer (Omicron Nanotechnology Ltd., Germany) with a monochromatic aluminium X-ray radiation source (1486.7 eV). Wide-scan surveys of all elements were performed, with subsequent high-resolution scans of the C 1s and O 1s. Relative sensitivity factors were used to evaluate the carbon-to-oxygen (C/O) ratios from the survey spectra. The samples were placed on a conductive carrier made from a high purity silver bar. An electron gun was used to eliminate sample charging during measurement (1–5 V).inVia Raman microscope (Renishaw, England) in backscattering geometry with CCD detector was used for Raman spectroscopy. DPSS laser (532 nm, 50 mW) with applied power of 5 mW and 50× magnification objective was used for the measurement. Instrument calibration was achieved with a silicon reference which gives a peak position at 520 cm^{-1} and a resolution of less than 1 cm^{-1}.

Thermal behaviour of prepared graphenes was analyzed by Simultaneous thermal analysis (STA). The DTA and TG curves were recorded simultaneously on a Linseis STA PT1600 apparatus at a heating rate of 10 °C min^{-1} in a dynamic air atmosphere (50 mL min^{-1}).

The surface area was measured using a sorption analyzer, Coulter SA 3100 (Backman Coulter). The samples were outgassed for 4 h at 95 °C under high vacuum (VALUE) prior to the sorption experiments. The reason for such a low temperature is to avoid degradation and further decomposition of oxygen functionalities. A TCD nitrogen cooled (77 K) detector was used for the evaluation of the results using BET (Brunauer, Emmett and Teller) and Kelvin equations.

X-ray powder diffraction data were collected at room temperature on Bruker D8 Discoverer powder diffractometer with parafocussing Bragg–Brentano geometry using CuK_α radiation (λ = 0.15418 nm, U = 40 kV, I = 40 mA). Data were scanned over the angular range 5°–90° (2θ) with a step size of 0.019° (2θ). Data evaluation was performed in the software package EVA.

Fourier transform infrared spectroscopy (FT-IR) measurements were performed on a NICOLET iS50R FTIR spectrometer (Thermo Scientific, USA) with DLaTGS detector in the range 4000–400 cm^{-1} at a resolution of 4 cm^{-1}.

The electrochemical characterization by means of cyclic voltammetry was performed using an potentiostat PGSTAT 204 (Metroohm Autolab B.V., The Netherlands). All glassy carbon electrodes were cleaned by polishing with an alumina suspension to renew the electrode surface then washed and wiped dry prior to any use. The samples were dispersed in DMF as the organic solvent to obtain a 1 mg/mL suspension. The suspension was then sonicated for 5 min at room temperature before every use. A cleaned GC electrode was then modified by coating with a 1.5 μL aliquot of the suspension and left to dry at ambient temperature to give a layer of randomly dispersed material on the GC surface. The modified GC electrodes, saturated Ag/AgCl reference electrode, and platinum counter electrode were then placed into an electrochemical cell which contains the electrolyte solution, and the measurements were then taken. The electrolytes used were 50 mM, pH 7.2 phosphate buffer solution (PBS) as the blank buffer electrolyte and 10 mM potassium ferrocyanide dissolved in PBS. All measurements were performed for three consecutive scans at a scan rate of 100 mV/s.

3. Results and discussion

Five different graphite oxides (GOs) were prepared by the Brodie, Hofmann, Hummers, Staudenmaier and Tour method (BRGO, HO-GO, HU-GO, ST-GO and TO-GO) [31–35]. The chemical composition of GOs was determined by energy dispersive spectroscopy, combustion elemental analysis and high resolution X-ray photoelectron spectroscopy (see the comparison of C/O ratios in Table SI-1and XPS survey spectra in Fig. SI-1). XPS was also used to calculate amount of individual oxygen functionalities of GOs (Table SI-2). GOs were further thermally or chemically reduced. The corresponding samples are termed according to their GO precursor and the type of reduction (thermally reduced graphene – TRG, chemically reduced graphenes – CRG). The process of oxidation and subsequent reduction is shown in Scheme 1. All samples

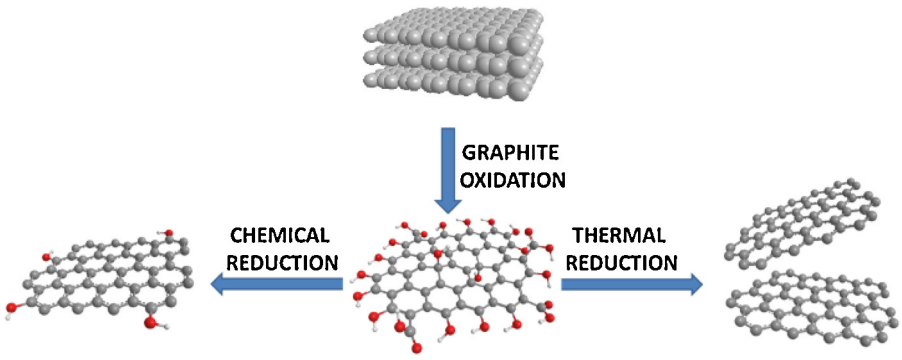

Scheme 1. Schematic drawing of the graphene synthesis procedures.

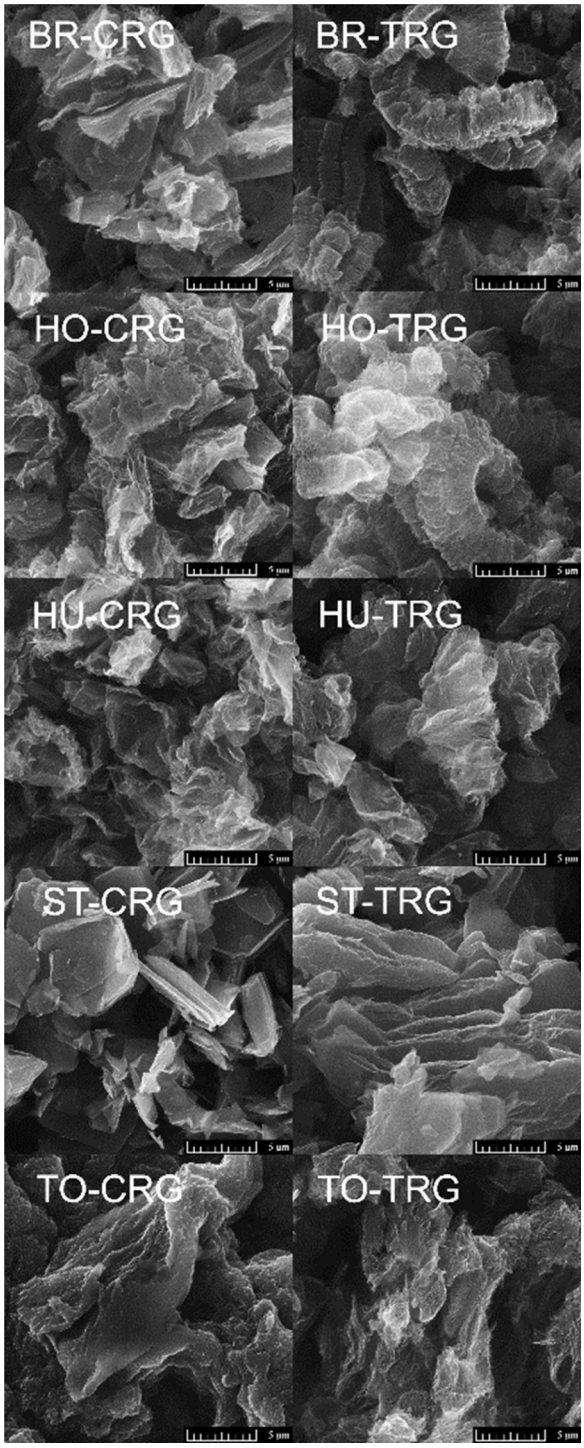

Fig. 1. The morphology of thermally and chemically reduced graphenes obtained by SEM. Scale bar corresponds to 5 μm.

were then analyzed by scanning electron microscopy (SEM), SEM-EDS, combustion elemental analysis (ECA), XPS, X-ray diffraction (XRD), surface area analysis (BET), Raman spectroscopy and simultaneous thermal analysis (STA) and cyclic voltammetry (CV). For more details, see Section 2.

The morphology of the obtained graphenes was investigated by SEM (Fig. 1). Much higher exfoliation level was observed for the thermally reduced graphenes compared to chemically reduced graphenes. Worm-like structure can be recognized in all thermally reduced graphenes. A notably lower exfoliation degree was found for samples BR-CRG and ST-CRG which can be explained by lower degree of oxidation of the starting graphite oxides. In the case of ST-TRG the morphology shows a sizably lower degree of expansion in comparison with other thermally reduced graphenes. This originates from low degree of oxidation and consequently has a significant effect on other properties discussed in the following paragraphs.

Table 1
The composition of chemically and thermally reduced graphene obtained by the elemental combustion analysis.

Sample	wt.% C	wt.% H	wt.% N	wt.% O
BR-CRG	75.17	1.83	1.17	21.83
HO-CRG	88.21	0.93	0.50	10.37
HU-CRG	82.53	0.73	2.52	14.23
ST-CRG	76.96	1.54	1.44	20.07
TO-CRG	71.67	1.62	5.59	21.13
BR-TRG	96.30	0.18	0.16	3.37
HO-TRG	97.09	0.36	0.00	2.55
HU-TRG	95.70	0.23	0.06	4.02
ST-TRG	95.59	0.09	0.17	4.15
TO-TRG	93.85	0.25	0.24	5.66

Table 2
C/O ratios (at.%) in chemically and thermally reduced graphenes obtained by SEM-EDS, ECA and XPS.

Sample	C/O SEM-EDS	C/O ECA	C/O XPS
BR-CRG	4.29	4.59	6.24
HO-CRG	10.90	11.33	10.14
HU-CRG	10.11	7.73	11.44
ST-CRG	5.73	5.11	9.79
TO-CRG	8.04	4.52	9.93
BR-TRG	14.54	38.07	12.09
HO-TRG	18.20	50.72	15.53
HU-TRG	26.54	31.71	22.64
ST-TRG	16.77	30.68	17.08
TO-TRG	29.88	22.09	28.67

In the next step, we analyzed the chemical composition using elemental analysis (see Table 1). The results confirmed our suggestions from SEM that the thermal reduction is much more effective compared to chemical reduction. The obtained C/O ratios are shown in Table 2. C/O ratios for chemically reduced graphenes were in the range between ~4 and ~11. On the other hand, the ratios for thermally reduced graphenes are much higher ranging from ~22 to ~50. The chemically reduced graphenes also contained higher amounts of nitrogen compared to thermally reduced graphenes. This originates from unintentional doping by nitrogen using hydrazine as a reduction agent. Moreover a significant amount of hydrogen can be observed in the chemically reduced graphene. Both these elements are introduced into graphene by hydrazine. Let us note that the formation of pyrazole heterocycle on the edges of graphene reduced by hydrazine was reported in literature [36]. The hydrogenation can originate from the reduction of ketone group to methylene group and alkaline cleavage of epoxy groups. The methylene group formation takes place preferentially on the sites where the pyrazole ring formation could not proceed due to the sterical reasons. Significant differences were observed for the thermally reduced graphene containing only negligible amount of nitrogen and hydrogen.

Due to the fact that elemental combustion analysis is not sensitive to precise measurement of oxygen content (indirect determination) we also analyzed samples using high resolution XPS. The XPS survey spectra are shown in Fig. SI-2, where C 1s is found at ~284.5 eV and O 1s is visible at ~533 eV. The survey spectra were used for the calculation of C/O ratios (Table 2). The obtained results confirmed the trends observed by CHN-O analysis. The lowest C/O ratios were obtained for chemically reduced samples (~5–10), while high C/O ratios were found for thermally reduced graphenes (~10–29), which is in good agreement with ECA. The highest C/O ratio was found for HU-TRG and TO-TRG

Table 3
Quantitative comparison (%) of individual carbon states of C 1s in graphenes obtained by high-resolution XPS.

Sample	C═C	C—C/C—H	C—O	C═O	O—C═O	π═π^*
BR-CRG	68.0	16.5	3.9	4.2	4.3	3.1
HO-CRG	56.3	25.5	8.4	3.2	3.2	3.4
HU-CRG	62.6	13.1	11.3	3.8	4.8	4.4
ST-CRG	69.8	14.4	6.3	4.5	2.1	2.9
TO-CRG	67.0	16.1	7.1	4.4	3.2	2.2
BR-TRG	65.0	15.5	5.9	6.3	4.8	2.5
HO-TRG	65.6	11.4	8.7	5.0	6.9	2.3
HU-TRG	70.9	12.3	5.8	3.3	4.4	3.4
ST-TRG	74.0	15.2	4.0	2.6	2.3	1.9
TO-TRG	69.9	12.9	6.3	4.1	4.0	2.8

synthesized from highly oxidized graphite oxides. Graphite oxide prepared by permanganate methods contains high concentration of thermally labile ketone and carboxylic acid functionalities which easily undergo decomposition under the formation of CO_2 and suppression of oxygen concentration. In comparison, the chlorate based graphite oxide contains predominantly hydroxyl functional groups which have significantly higher thermal stability. Despite the fact that higher amount of nitrogen was found by ECA analysis for CRG-graphenes, lower nitrogen content was detected by XPS except for HU-CRG and TO-CRG sample which contained 0.95 at.% and 2.58 at.% of nitrogen, respectively. The results are summarized in Supporting Information (Table SI-3).

Details of high-resolution XPS details of C1 s spectra were used to quantify the presence of individual carbon states: C═C (284.4 eV); C—C/C—H (285.4 eV); C—O (286.3 eV); C═O (288.0 eV); O—C═O (289.0 eV) and π–π^* interaction (290.5 eV). The obtained fit is shown in Fig. 2, while the quantitative composition of C 1s individual states is in Table 3, while the detailed fitting of C 1s peak is shown in Fig. SI-4. The results of regression analysis are in good agreement to the overall chemical composition obtained by XPS.

In addition, the chemical composition was also studied by SEM-EDS. Except for C and O, low concentrations of K, Mn, S and Cl (maximally 0.2 wt.%) were detected. These impurities originate from the chemicals used for synthesis of graphite oxide and persist also in graphene after its reduction. Also in this case we calculated C/O ratios (Table 2). The results are similar to those obtained from XPS, slightly differing from the ECA data. The chemically reduced graphenes exhibited the C/O ratio between ~4 and 11 while the thermally reduced graphenes had the C/O ratios in the range ~14–30. HU-TRG and TO-TRG revealed the highest C/O ratio, which is in good agreement with XPS data.

According to the comparison of C/O ratios acquired by SEM-EDS, ECA and XPS the C/O values for CRG-graphenes were very similar to each other, but always lower than TRG-graphenes for all samples. The C/O ratio acquired by ECA differs from those obtained from XPS and SEM-EDS due to indirect determination of oxygen content and also due to different sensitivities of these methods. The XPS analytical technique is sensitive towards first few nanometers of the surface and EDS analysis needs fully dense flat samples for optimal performance. However the general trends confirmed by these three methods are in good agreement.

Knowing the chemical composition of graphenes, we studied their structure using XRD (Fig. 3). The position of (002) reflection was found at higher values of 2θ compared to graphite, where the interlayer distance is 3.356 Å (Table 4) [27]. Slightly higher interlayer distances were found for chemically reduced graphenes due to remaining functional groups, which contribute to the enlargement of interlayer distance. The highest interlayer distances were found for HU-CRG and TO-CRG. These samples originated from highly oxidized graphite oxides, but they were reduced by less effective chemical reduction, hence a huge number of oxygen containing groups remained between the layers and, moreover,

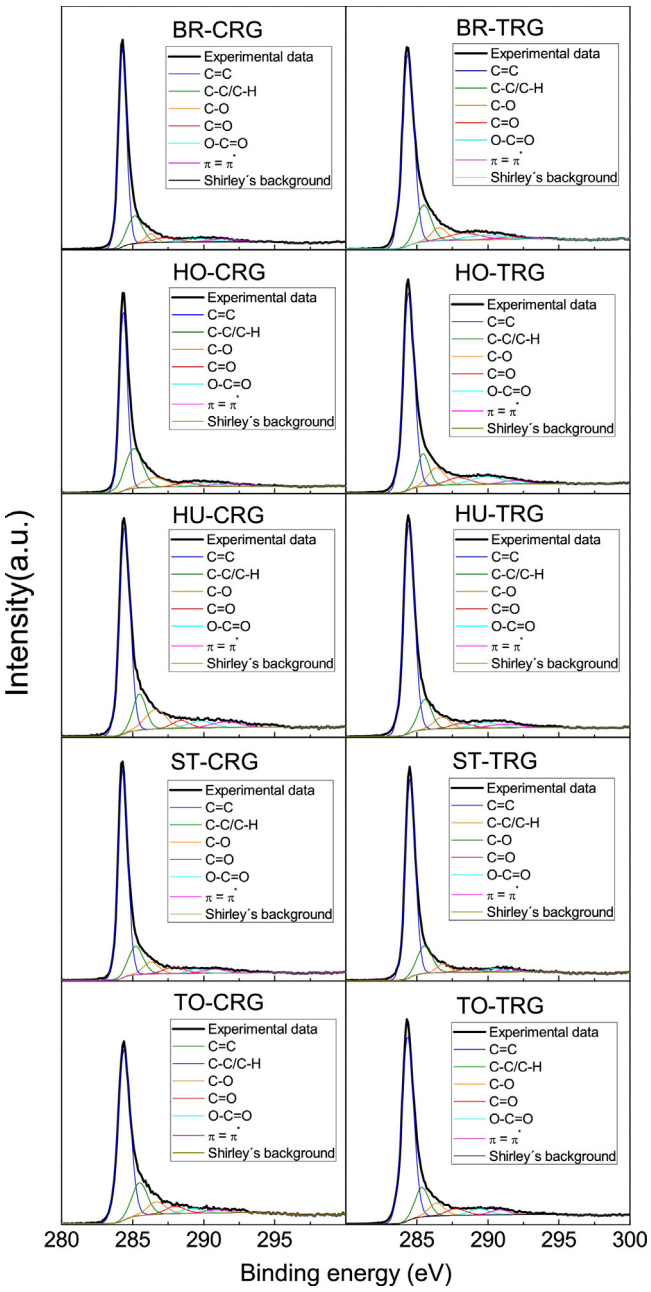

Fig. 2. High-resolution XPS detail of C 1s with fittings corresponding to individual carbon states of chemically and thermally reduced graphene.

nitrogen containing groups were also attached to the graphene surface. The disorder within graphene can be also investigated by XRD and the FWHM of (002) reflection can be correlated with the average number of layers [27]. The average number of layers can be evaluated from Scherer formula providing the mean crystallite size. For (002) reflection the size (thickness of the sheets) is proportional to the number of the layers. The results are summarized in Table 4. The correlation between the average number of layers in graphene and the degree of graphite oxidation is clearly visible. The highest average thickness was observed for graphene prepared by Staudenmaier method and on the opposite the lowest number of layers corresponding to the highest degree of exfoliation was observed on graphene prepared from graphite oxide originating from permanganate methods (TO-GO and HU-GO). The asymmetric shape of (002) reflection of graphene prepared from BR-GO may indicate an inhomogeneous or incomplete oxidation of graphite which led to a formation of graphene with different degree of exfoliation.

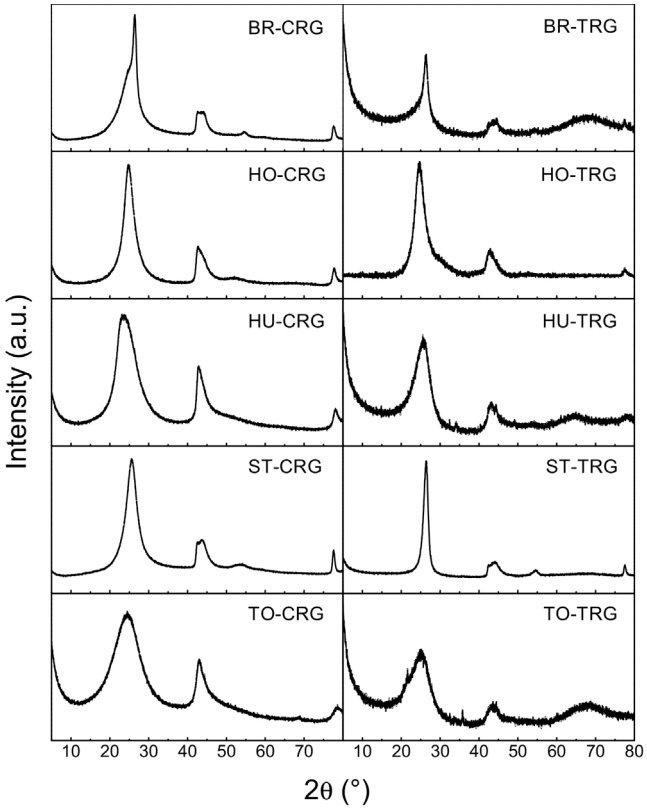

Fig. 3. XRD diffraction patterns of graphenes prepared by chemical and thermal reduction.

Table 4
Interlayer distance of graphenes prepared by chemical and thermal reduction obtained by XRD.

Sample	Interlayer distance (Å)	Number of layers
BR-CRG	3.369	10
HO-CRG	3.595	5
HU-CRG	3.745	3
ST-CRG	3.467	6–7
TO-CRG	3.632	2–3
BR-TRG	3.372	5–6
HO-TRG	3.597	5
HU-TRG	3.446	3
ST-TRG	3.372	13–14
TO-TRG	3.538	2–3

Table 5
D/G ratios of chemically and thermally reduced graphenes measured by Raman spectroscopy.

Sample	D/G ratio
BR-CRG	1.11
HO-CRG	1.27
HU-CRG	1.17
ST-CRG	1.09
TO-CRG	0.98
BR-TRG	1.16
HO-TRG	1.22
HU-TRG	1.32
ST-TRG	1.11
TO-TRG	1.14

To obtain more information about the structure and defect density of the graphenes, Raman spectroscopy was used (Fig. SI-3). Two major bands, D-band and G-band, were found for all samples [37]. The presence of the D-band (1350 cm^{-1}) indicates defects in the graphene layer, while the G-band (1580 cm^{-1}) represents

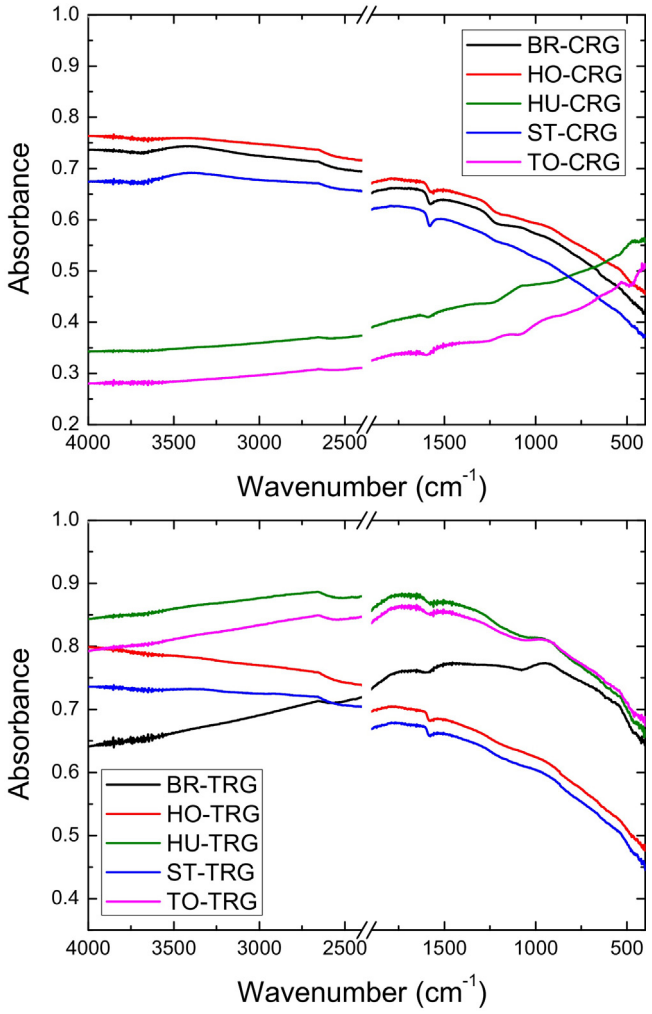

Fig. 4. FT-IR spectra of chemically and thermally reduced graphenes.

Table 6
Surface areas of graphenes prepared by chemical and thermal reduction obtained by BET.

Sample	Surface area ($m^2\ g^{-1}$)
BR-CRG	13.7
HO-CRG	25.0
HU-CRG	247.0
ST-CRG	5.5
TO-CRG	559.6
BR-TRG	626.2
HO-TRG	781.0
HU-TRG	533.8
ST-TRG	25.4
TO-TRG	578.8

sp^2 bonded carbon atoms in the graphene layer (non-defected area) [38]. We calculated D/G ratios indicting the density of defects (Table 5). The obtained D/G ratios for all samples were between 0.98 and 1.32. A slightly higher density of defects was obtained for thermally reduced graphenes originating from a formation of large amount of defects within graphene sheets by thermal decomposition of oxygen functionalities.

Surface area of graphenes was measured by sorption techniques. The theoretical surface of a single-layer graphene is supposed to be 2630 $m^2\ g^{-1}$ [1]. The thermally reduced graphenes had much higher surface area compared to chemically reduced graphenes (Table 6). The lowest surface area was found for samples ST-CRG and ST-TRG (5.5 $m^2\ g^{-1}$ and 25.4 $m^2\ g^{-1}$) due to a low degree

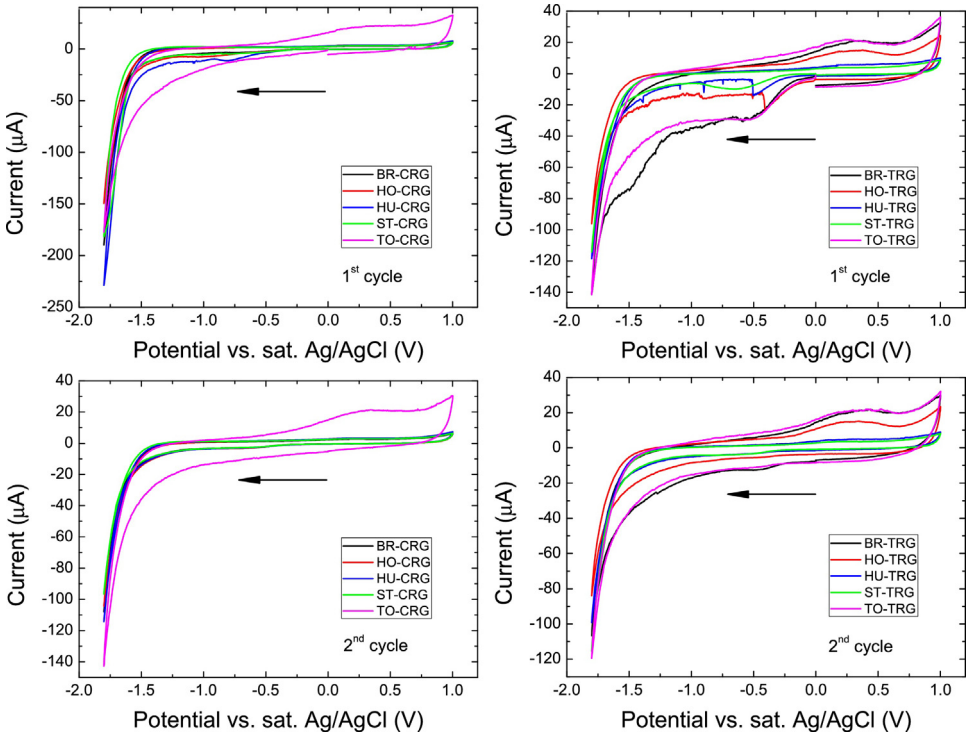

Fig. 5. Inherent electrochemistry (1st and 2nd cycle) of graphenes prepared by chemical and thermal reduction measured in PBS (50 mM, pH 7.2, scan rate 100 mV/s).

of oxidation. The low surface areas were also observed also on other chemically reduced graphite oxides (BR-CRG and HO-CRG) prepared by chlorate methods. On the other hand, chemically reduced graphene originating from graphite oxide prepared by permanganate methods exhibit surfaces that are comparable to thermally reduced graphene. The sample TO-CRG had a surface area of 559.6 $m^2 g^{-1}$ and HU-CRG 247.0 $m^2 g^{-1}$. The differences in surface area of chemically reduced graphenes indicate a significant role of graphite oxide composition as well as the type of oxygen functionalities. The high concentration of ketone groups together with high degree of oxidation can increase the surface area of chemically reduced graphene by two orders of magnitude. For the case of thermally reduced graphene the differences are significantly lower with the exception of ST-TRG which had one order of magnitude lower surface area due to the low degree of oxidation of the starting graphite oxide (ST-GO). In the case of thermally reduced graphene any clear correlation between the surface area and the chemical composition of starting graphite oxide was not observed. In general, high surface areas (534–781 $m^2 g^{-1}$) were found for TO-CRG, BR-TRG, HO-TRG, HU-TRG and TO-TRG. Such high surface areas originate from the thermal reduction process, where the oxygen functionalities are decomposed into gaseous products invoking an extreme pressure in the interlayer space and exfoliating the graphite oxide into graphene. Hence a characteristic expanded structure as observed on SEM images was formed exhibiting a high surface as measured by BET method.

In order to characterize remaining oxygen functionalities the FT-IR was measured for both starting graphite oxides (Fig. SI-4) and reduced graphenes (Fig. 4). Graphite oxides showed a number of oxygen functionalities except of ST-GO, which confirmed relatively low oxidation rate of this sample. Graphite oxides revealed a broad absorption band of O—H stretching originating from hydroxyls functional groups around 3400 cm^{-1} [39]. The C=O vibration band in carboxylic acid was found at 1720 cm^{-1} [40]. The vibration band of C—O functionalities was observed around 1220 cm^{-1} and 1060 cm^{-1} [39]. After the reduction, the number of oxygen functionalities dramatically decreased confirming successful reduction by both methods; higher reduction rate was achieved by the thermal reduction. The stretching of C=C bonds was clearly visible at 1630 cm^{-1}; but other bands almost disappeared [40].

Thermal stability of graphenes was tested using simultaneous thermal analysis (STA) in dynamic air atmosphere (Fig. SI-5). The thermal analysis confirmed a successful reduction of all graphenes while the exfoliation peak which is usually found at ~200 °C was not detected in any sample [41]. Slight changes in the sample mass were observed in the range of 200–300 °C for the chemically reduced graphene indicating thermal decomposition of some thermally labile oxygen functionalities. Interestingly, this effect was observed only for samples prepared by chlorate methods. At the temperatures over 400 °C, one large exothermic effect was observed originating from oxidation/combustion of graphene. The onset temperatures of oxidation/combustion of graphenes are shown in Table 7. The thermal stability of thermally reduced graphenes is approximately 100 °C higher than that of chemically reduced graphenes. This effect can be correlated with the higher concentration of remaining oxygen functionalities in the chemically reduced graphene which contribute to the reduction of its thermal stability in oxidation atmosphere. The difference was significantly lower only for samples ST-CRG and ST-TRG due to the extremely low surface corresponding to low degree of exfoliation. In general graphene is stable towards oxidation up to 400 °C and this temperature can be increased by a suppression of the remaining oxygen functionalities concentration.

Inherent electrochemistry (that is, redox properties of graphene itself) was measured by means of cyclic voltammetry to obtain more information about the composition of the remaining oxygen containing functionalities (Fig. 5). It was described in literature that the peroxide groups reduction potential is around −0.7 V, aldehyde around −1.0 V, epoxide around −1.5 V and carboxyl around −2.0 V (stated vs. Ag/AgCl) [40]. For all samples there were no significant reduction maxima which confirmed a successful reduction: these samples did not contain any remaining electrochemically active oxygen functionalities. Significant differences can be observed between the stability towards anodic oxidation of chemically

Table 7
Onset temperatures of oxidation/combustion of graphenes prepared by chemical and thermal reduction.

Sample	Temperature (°C)
BR-CRG	422
HO-CRG	398
HU-CRG	400
ST-CRG	574
TO-CRG	404
BR-TRG	532
HO-TRG	566
HU-TRG	505
ST-TRG	598
TO-TRG	536

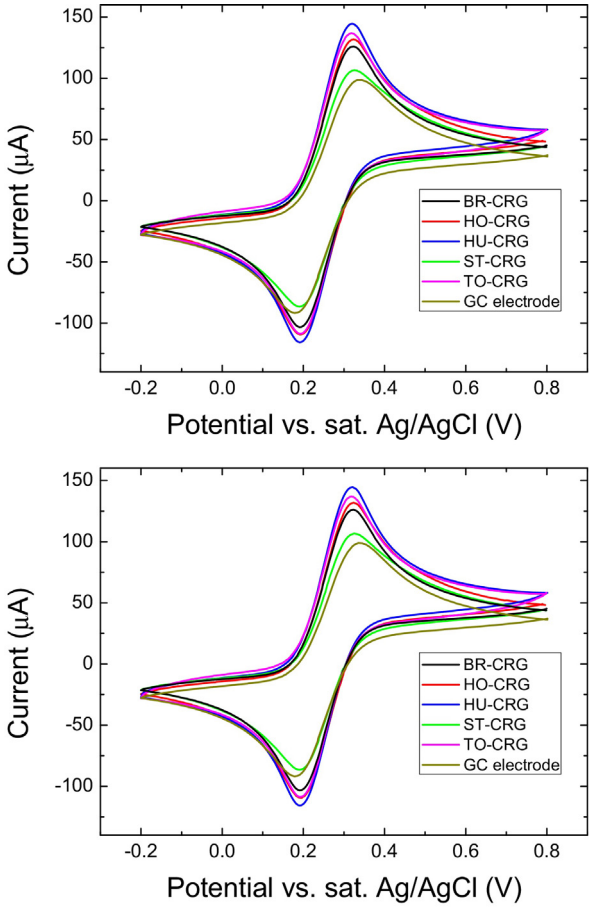

Fig. 6. Cyclic voltammogram of chemically and thermally reduced graphenes. Scan rate 100 mV s^{-1}, 50 mM PBS (pH 7.2) with 10 mM $K_4[Fe(CN)_6]$.

reduced graphenes. The oxidation peak with a maximum around +0.3 V was observed on the chemically reduced graphene prepared from graphite oxide oxidized by permanganate methods. In the case of thermally reduced graphene the oxidation peak was observed for all samples. The reversible oxidation of graphene prepared from graphite oxidized by permanganate methods has been also recently reported in literature [42]. However, the onset of this oxidation process is almost independent on the type of graphene, the oxidation current and also the maxima are slightly shifted for different TRG sample. It is possible to correlate the oxidation current with the surface area of graphene measured by BET; higher oxidation currents are observed for the samples with high surface area.

The cyclic voltammetry was performed with $[Fe(CN)_6]^{3-/4-}$ redox probe to compare heterogeneous electron transfer (HET) rate (Fig. 6). The HET rate represented by the value of peak-to-peak separation is an important parameter for a broad range of graphene applications in energy storage and conversion devices. The observed values of HET rate represented by peak-to-peak separation range between 123 and 154 mV and are shown in Table 8. The thermally reduced graphenes showed better performance compared to chemically reduced graphenes, however, the difference was relatively small. This suggests that both reduction methods are suitable for preparation of graphene with fast heterogeneous electron transfer which is important for various electrocatalytic processes and construction of electrochemical sensors.

Table 8
Peak-to-peak separation values corresponding to HET rate for graphenes prepared by chemical and thermal reduction.

Sample	Peak-to-peak separation (mV)	Ox/red pot. (mV)
BR-CRG	130	322/192
HO-CRG	129	323/194
HU-CRG	129	321/192
ST-CRG	135	326/191
TO-CRG	125	318/193
BR-TRG	154	335/181
HO-TRG	136	325/189
HU-TRG	126	320/194
ST-TRG	123	319/196
TO-TRG	126	318/192
GC electrode	161	340/179

4. Conclusions

The influence of oxidation methods on the properties of chemically and thermally reduced graphene was investigated in detail. Five main methods for the synthesis of graphite oxide using chlorate and permanganate oxidation procedures were selected for the investigation. Our findings show several significant differences in the graphenes prepared by chlorate and permanganate methods. In general, the properties like surface area, morphology and remaining oxygen functionalities are controlled not only by the degree of oxidation, but also by the composition of oxygen functionalities and the method of reduction. In general the thermal reduction methods yield significantly higher degree of exfoliation and lower concentration of oxygen functionalities. Differences between the individual samples are significantly lower in such graphenes in comparison with various graphenes prepared by chemical reduction. This mainly originates from incomparably lower concentration of oxygen functionalities and much higher C/O ratio indicating the degree of reduction. The exfoliation of chemically reduced graphene is significantly higher for the samples originating from graphite oxide prepared by permanganate routes compared to chlorate methods, showing the importance of proper selection of the starting graphite oxide for various applications. The main exception from all trends is the graphene prepared from graphite oxidized by Staudenmaier method. The low degree of oxidation led to a markedly lower degree of exfoliation and subsequently to high differences in the observed properties such as surface area, stability towards oxidation and others. Interestingly, all graphenes have comparable HET rate represented by the value of peak-to-peak separation value using hexakyanoferrate redox probe. Our findings showed large variability in structure, composition and properties of graphene obtained from graphite oxide prepared by various oxidation methods. These findings must be considered for the proper selection of graphene for different applications of graphene in industrial processes.

Acknowledgements

The project was supported by Czech Science Foundation (GACR No. 15-09001S and 16-05167S) and by financial support from Specific University Research (MSMT No 20-SVV/2016).

Appendix A. Supplementary data

Supplementary data associated with this article can be found, in the online version, at doi:10.1016/j.apmt.2016.06.001.

References

[1] A.K. Geim, K.S. Novoselov, The rise of graphene, Nat. Mater. 6 (2007) 183–191.
[2] Y. Zhang, T.-T. Tang, C. Girit, Z. Hao, M.C. Martin, A. Zettl, M.F. Crommie, Y.R. Shen, F. Wang, Direct observation of a widely tunable bandgap in bilayer graphene, Nature 459 (2009) 820–823.
[3] M. Katsnelson, K. Novoselov, A. Geim, Chiral tunnelling and the Klein paradox in graphene, Nat. Phys. 2 (2006) 620–625.
[4] X. Wang, L. Zhi, K. Müllen, Transparent, conductive graphene electrodes for dye-sensitized solar cells, Nano Lett. 8 (2008) 323–327.
[5] K.S. Novoselov, V. Fal, L. Colombo, P. Gellert, M. Schwab, K. Kim, A roadmap for graphene, Nature 490 (2012) 192–200.
[6] F. Bonaccorso, Z. Sun, T. Hasan, A. Ferrari, Graphene photonics and optoelectronics, Nat. Photonics 4 (2010) 611–622.
[7] N. Yang, J. Zhai, D. Wang, Y. Chen, L. Jiang, Two-dimensional graphene bridges enhanced photoinduced charge transport in dye-sensitized solar cells, ACS Nano 4 (2010) 887–894.
[8] R. Giardi, S. Porro, T. Topuria, L. Thompson, C.F. Pirri, H.-C. Kim, One-pot synthesis of graphene-molybdenum oxide hybrids and their application to supercapacitor electrodes, Appl. Mater. Today 1 (2015) 27–32.
[9] X.-X. Ma, X.-Q. He, Cobalt oxide anchored on nitrogen and sulfur dual-doped graphene foam as an effective oxygen electrode catalyst in alkaline media, Appl. Mater. Today 4 (2016) 1–8.
[10] X. Deng, L. Lü, H. Li, F. Luo, The adsorption properties of Pb(II) and Cd(II) on functionalized graphene prepared by electrolysis method, J. Hazard. Mater. 183 (2010) 923–930.
[11] O. Jankovský, P. Šimek, K. Klímová, D. Sedmidubský, M. Pumera, Z. Sofer, Highly selective removal of Ga^{3+} ions from Al^{3+}/Ga^{3+} mixtures using graphite oxide, Carbon 89 (2015) 121–129.
[12] R.K. Joshi, S. Alwarappan, M. Yoshimura, V. Sahajwalla, Y. Nishina, Graphene oxide: the new membrane material, Appl. Mater. Today 1 (2015) 1–12.
[13] A. Martinez, K. Fuse, S. Yamashita, Mechanical exfoliation of graphene for the passive mode-locking of fiber lasers, Appl. Phys. Lett. 99 (2011) 121107.
[14] A.N. Obraztsov, Chemical vapour deposition: making graphene on a large scale, Nat. Nanotechnol. 4 (2009) 212–213.
[15] M.D. Stoller, S. Park, Y. Zhu, J. An, R.S. Ruoff, Graphene-based ultracapacitors, Nano Lett. 8 (2008) 3498–3502.
[16] C. Liu, Z. Yu, D. Neff, A. Zhamu, B.Z. Jang, Graphene-based supercapacitor with an ultrahigh energy density, Nano Lett. 10 (2010) 4863–4868.
[17] L. Qu, Y. Liu, J.-B. Baek, L. Dai, Nitrogen-doped graphene as efficient metal-free electrocatalyst for oxygen reduction in fuel cells, ACS Nano 4 (2010) 1321–1326.
[18] C.H.A. Wong, O. Jankovský, Z. Sofer, M. Pumera, Vacuum-assisted microwave reduction/exfoliation of graphite oxide and the influence of precursor graphite oxide, Carbon 77 (2014) 508–517.
[19] P. Šimek, Z. Sofer, O. Jankovský, D. Sedmidubský, M. Pumera, Graphene: oxygen-free highly conductive graphene papers, Adv. Funct. Mater. 24 (2014) 4877.
[20] S. Stankovich, D.A. Dikin, R.D. Piner, K.A. Kohlhaas, A. Kleinhammes, Y. Jia, Y. Wu, S.T. Nguyen, R.S. Ruoff, Synthesis of graphene-based nanosheets via chemical reduction of exfoliated graphite oxide, Carbon 45 (2007) 1558–1565.
[21] X. Gao, J. Jang, S. Nagase, Hydrazine and thermal reduction of graphene oxide: reaction mechanisms, product structures, and reaction design, J. Phys. Chem. C 114 (2009) 832–842.
[22] A.B. Bourlinos, D. Gournis, D. Petridis, T. Szabó, A. Szeri, I. Dékány, Graphite oxide: chemical reduction to graphite and surface modification with primary aliphatic amines and amino acids, Langmuir 19 (2003) 6050–6055.
[23] O. Jankovský, P. Šimek, J. Luxa, D. Sedmidubský, I. Tomandl, A. Macková, R. Mikšová, P. Malinský, M. Pumera, Z. Sofer, Definitive insight into the graphite oxide reduction mechanism by deuterium labeling, ChemPlusChem 80 (2015) 1399–1407.
[24] O. Jankovský, P. Šimek, M. Nováček, J. Luxa, D. Sedmidubský, M. Pumera, A. Macková, R. Mikšová, Z. Sofer, Use of deuterium labelling – evidence of graphene hydrogenation by reduction of graphite oxide using aluminium in sodium hydroxide, RSC Adv. 5 (2015) 18733–18739.
[25] Z. Sofer, O. Jankovský, A. Libánská, P. Šimek, M. Nováček, D. Sedmidubský, A. Macková, R. Mikšová, M. Pumera, Definitive proof of graphene hydrogenation by Clemmensen reduction: use of deuterium labeling, Nanoscale 7 (2015) 10535–10543.
[26] V.H. Pham, H.D. Pham, T.T. Dang, S.H. Hur, E.J. Kim, B.S. Kong, S. Kim, J.S. Chung, Chemical reduction of an aqueous suspension of graphene oxide by nascent hydrogen, J. Mater. Chem. 22 (2012) 10530–10536.
[27] Z. Sofer, P. Šimek, O. Jankovský, D. Sedmidubský, P. Beran, M. Pumera, Neutron diffraction as a precise and reliable method for obtaining structural properties of bulk quantities of graphene, Nanoscale 6 (2014) 13082–13089.
[28] B. Zhao, P. Liu, Y. Jiang, D. Pan, H. Tao, J. Song, T. Fang, W. Xu, Supercapacitor performances of thermally reduced graphene oxide, J. Power Sources 198 (2012) 423–427.
[29] O. Jankovsky, S. Hrdlickova Kuckova, M. Pumera, P. Simek, D. Sedmidubsky, Z. Sofer, Carbon fragments are ripped off from graphite oxide sheets during their thermal reduction, New J. Chem. 38 (2014) 5700–5705.
[30] Z. Sofer, O. Jankovský, P. Simek, D. Sedmidubsky, J. Šturala, J. Kosina, R. Mikšová, A. Macková, M. Mikulics, M. Pumera, Insight into the mechanism of the thermal reduction of graphite oxide: deuterium-labeled graphite oxide is the key, ACS Nano 9 (2015) 5478–5485.
[31] B.C. Brodie, On the atomic weight of graphite, Philos. Trans. R. Soc. Lond. 149 (1859) 249–259.
[32] U. Hofmann, A. Frenzel, Die Reduktion von Graphitoxyd mit Schwefelwasserstoff, Kolloid-Z. 68 (1934) 149–151.
[33] W. Hummers, R. Offeman, Preparation of graphitic oxide, J. Am. Chem. Soc. 80 (1958) 1339.
[34] L. Staudenmaier, Verfahren zur Darstellung der Graphitsäure, Ber. Dtsch. Chem. Ges. 31 (1898) 1481–1487.
[35] D.C. Marcano, D.V. Kosynkin, J.M. Berlin, A. Sinitskii, Z. Sun, A. Slesarev, L.B. Alemany, W. Lu, J.M. Tour, Improved synthesis of graphene oxide, ACS Nano 4 (2010) 4806–4814.
[36] S. Park, Y. Hu, J.O. Hwang, E.-S. Lee, L.B. Casabianca, W. Cai, J.R. Potts, H.-W. Ha, S. Chen, J. Oh, S.O. Kim, Y.-H. Kim, Y. Ishii, R.S. Ruoff, Chemical structures of hydrazine-treated graphene oxide and generation of aromatic nitrogen doping, Nat. Commun. 3 (2012) 638.
[37] D.R. Dreyer, R.S. Ruoff, C.W. Bielawski, From conception to realization: an historial account of graphene and some perspectives for its future, Angew. Chem. Int. Ed. 49 (2010) 9336–9344.
[38] M.S. Dresselhaus, A. Jorio, M. Hofmann, G. Dresselhaus, R. Saito, Perspectives on carbon nanotubes and graphene Raman spectroscopy, Nano Lett. 10 (2010) 751–758.
[39] M. Mermoux, Y. Chabre, A. Rousseau, FTIR and ^{13}C NMR study of graphite oxide, Carbon 29 (1991) 469–474.
[40] S. Stankovich, R.D. Piner, S.T. Nguyen, R.S. Ruoff, Synthesis and exfoliation of isocyanate-treated graphene oxide nanoplatelets, Carbon 44 (2006) 3342–3347.
[41] O. Jankovský, D. Sedmidubský, P. Šimek, K. Klímová, D. Bouša, C. Boothroyd, A. Macková, Z. Sofer, Separation of thorium ions from wolframite and scandium concentrates using graphene oxide, Phys. Chem. Chem. Phys. 17 (2015) 25272–25277.
[42] A.Y.S. Eng, A. Ambrosi, C.K. Chua, F. Šaněk, Z. Sofer, M. Pumera, Unusual inherent electrochemistry of graphene oxides prepared using permanganate oxidants, Chem. Eur. J. 19 (2013) 12673–12683.